Vacuum polarization and finite-nuclear-size effects in the two-photon decay of hydrogenlike ions

J. Sommerfeldt,[1,2] R. A. Müller,[1,2] A. V. Volotka,[3] S. Fritzsche,[3,4] and A. Surzhykov[1,2]

[1]*Physikalisch-Technische Bundesanstalt, D-38116 Braunschweig, Germany*
[2]*Technische Universität Braunschweig, D-38106 Braunschweig, Germany*
[3]*Helmholtz Institute Jena, D-07743 Jena, Germany*
[4]*Theoretisch-Physikalisches Institut, Friedrich-Schiller-Universität Jena, D-07743 Jena, Germany*

(Received 7 August 2020; accepted 25 September 2020; published 13 October 2020)

The total two-photon decay rate of hydrogenlike ions is studied using relativistic quantum electrodynamics. In particular, we analyze how finite nuclear size and QED vacuum polarization corrections affect the decay rate. To calculate these corrections, a finite basis set method based on B splines is used for the generation of quasicomplete atomic spectra and, hence, of the relativistic Green's function. By making use of this B-spline approach, high precision calculations have been performed for the $2s_{1/2} \to 1s_{1/2} + 2\gamma$ and $2p_{1/2} \to 1s_{1/2} + 2\gamma$ decay of hydrogenlike ions along the entire isoelectronic sequence. The results of these calculations show that both QED and finite nuclear size effects are comparatively weak for the $2s_{1/2} \to 1s_{1/2} + 2\gamma$ transition. In contrast, they are much more pronounced for the $2p_{1/2} \to 1s_{1/2} + 2\gamma$ decay, where, for hydrogenlike uranium, the decay rate is reduced by 0.484% due to the finite nuclear size and enhanced by 0.239% if the vacuum polarization is taken into account.

DOI: 10.1103/PhysRevA.102.042811

I. INTRODUCTION

Theoretical investigations of two-photon transitions in hydrogenlike ions have a long history going back to the seminal work by Göppert-Mayer [1]. In that work, solutions of the nonrelativistic Schrödinger equation have been applied to calculate the rate of the $2s \to 1s$ two-photon transition in neutral hydrogen. Four decades later, the first fully relativistic calculations were done to describe the two-photon decay of the metastable $2s_{1/2}$ state [2,3]. Being performed within the framework of second-order perturbation theory for the electron-photon coupling, these calculations are rather demanding. They require a representation of the entire atomic spectrum including the positive and negative continuum. Theoretical investigations of two-photon transitions in hydrogenlike ions therefore have become a testbed for the development of second-order computational approaches. Several such methods have been developed during the past decades leading to more precise predictions of the decay rates [4–6]. The increased accuracy of the calculations has allowed one to investigate how the total and differential rates are influenced by nuclear and even QED effects. In particular, finite nuclear size and mass corrections to the two-photon decay of $n = 2$ hydrogenic states have been studied [7–10]. Furthermore, QED effects have been discussed to all orders in αZ for one-photon transitions [11–13] but only to the leading order for the two-photon decay of hydrogenlike ions [14,15].

Despite the recent interest in high-precision calculations of two-photon transitions in hydrogenlike ions, no systematic fully relativistic analysis of the finite nuclear size and QED corrections to the decay rates has been performed. To the best of our knowledge, the first steps towards this analysis were done by Parpia and Johnson [9] who have discussed the finite nuclear size corrections for the $2s_{1/2} \to 1s_{1/2} + 2\gamma$ transition in dipole approximation. Moreover, in the work by Labzowsky *et al.* [10], calculations with a finite nucleus have been performed but with low relative precision. More accurate calculations of two-photon transitions in hydrogenic systems are required, however, to get a more complete picture of bound electronic states and as benchmark data for future second-order atomic calculations.

In this contribution, therefore, we present a theoretical study of the finite nuclear size and QED vacuum polarization corrections to the two-photon decay rate of hydrogenlike ions. To analyze these effects, we employ the relativistic quantum electrodynamics approach whose basic equations are recalled in Sec. II A. In Sec. II B, we discuss the finite basis set method used to construct the second-order transition matrix element. The implementation of this method requires knowledge about the electron-nucleus interaction potential. In Sec. II C, we show how this potential can be modified from the pure Coulombic case to include finite nuclear size and vacuum polarization effects. Since we aim for a discussion of small effects, the accuracy of the two-photon calculations should be sufficiently high. In Sec. III, we discuss how such accuracy can be achieved by using quadruple precision arithmetic. The results of our calculations are presented in Sec. IV for the $2s_{1/2} \to 1s_{1/2} + 2\gamma$ and $2p_{1/2} \to 1s_{1/2} + 2\gamma$ decay of hydrogenlike ions in the range from $Z = 1$ to $Z = 92$. The results of these calculations are in good agreement with previous predictions and indicate that the finite nuclear size and QED corrections to the decay rate are of opposite sign. We found that the finite nuclear size reduces the decay rates while the vacuum polarization enhances them. Both effects are more

 ©2020 American Physical Society

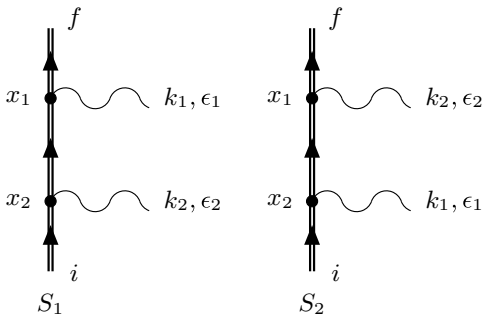

FIG. 1. Leading order Feynman graphs corresponding to the two-photon transition $|i\rangle \to |f\rangle + \gamma(k_1, \epsilon_1) + \gamma(k_2, \epsilon_2)$.

pronounced for the $2p_{1/2} \to 1s_{1/2} + 2\gamma$ transition compared to the $2s_{1/2} \to 1s_{1/2} + 2\gamma$ case. The summary of these results and outlook are finally given in Sec. V. Relativistic units $\hbar = m_e = c = 1$ are used throughout this paper if not stated otherwise.

II. THEORY

A. QED description of two-photon decay

Within the framework of quantum electrodynamics, two-photon decay of hydrogenlike ions can be described, to the leading order, by the two Feynman diagrams presented in Fig. 1. As usual, in these diagrams the wavy lines display photons emitted with wave vectors k_1, k_2 and polarization vectors ϵ_1, ϵ_2. Moreover, the double straight lines display the bound electron which proceeds from the initial $|i\rangle = |n_i\kappa_i\mu_i\rangle$ to the final $|f\rangle = |n_f\kappa_f\mu_f\rangle$ hydrogenic state. Here, n is the principal quantum number, κ is the Dirac quantum number, and μ is the projection of the total angular momentum $j = |\kappa| - \frac{1}{2}$.

By using the Feynman correspondence rules, we can write the S matrix element for each diagram from Fig. 1. For example, the matrix element for the first diagram is given by

$$S_1 = (-ie)^2 \int d^4x_1 \int d^4x_2\, \bar{\phi}_f(x_1)\gamma^{\mu_1} A^*_{\mu_1}(x_1) \times S_F(x_1, x_2)\gamma^{\mu_2}\phi_i(x_2)A^*_{\mu_2}(x_2), \quad (1)$$

where S_F is the Feynman propagator

$$S_F(x_1, x_2) = \frac{1}{2\pi i}\int_{-\infty}^{\infty} dw \sum\!\!\!\!\!\!\int_{\nu} \frac{\phi_\nu(\boldsymbol{x}_1)\bar{\phi}_\nu(\boldsymbol{x}_2)}{E_\nu + w(1 + i\delta)} e^{iw(t_1 - t_2)}, \quad (2)$$

and the ϕ_i and ϕ_f are solutions of the relativistic Dirac equation with corresponding eigenenergies E_i and E_f [16]. Here, the summation over the intermediate states $|\nu\rangle = |n_\nu\kappa_\nu\mu_\nu\rangle$ is understood as a sum over all bound states and an integral over the positive and negative continuum.

By constructing the S matrix element for the second Feynman diagram in a similar way, inserting the electron and photon wave functions and carrying out the integration over time and frequency explicitly we obtain

$$S_1 + S_2 = -\frac{4\pi^2 ie^2}{\sqrt{\omega_1\omega_2}} M_{fi}(\boldsymbol{k}_1, \boldsymbol{\epsilon}_1, \boldsymbol{k}_2, \boldsymbol{\epsilon}_2), \quad (3)$$

where the matrix element M_{fi} is given by

$$M_{fi}(\boldsymbol{k}_1, \boldsymbol{\epsilon}_1, \boldsymbol{k}_2, \boldsymbol{\epsilon}_2) = \sum_\nu \frac{\langle f|\,\hat{R}^\dagger(\boldsymbol{k}_1, \boldsymbol{\epsilon}_1)\,|\nu\rangle\,\langle\nu|\,\hat{R}^\dagger(\boldsymbol{k}_2, \boldsymbol{\epsilon}_2)\,|i\rangle}{E_\nu - E_i + \omega_2} + \frac{\langle f|\,\hat{R}^\dagger(\boldsymbol{k}_2, \boldsymbol{\epsilon}_2)\,|\nu\rangle\,\langle\nu|\,\hat{R}^\dagger(\boldsymbol{k}_1, \boldsymbol{\epsilon}_1)\,|i\rangle}{E_\nu - E_i + \omega_1}. \quad (4)$$

Here, the wave and polarization vectors are now given as 3-vectors since we have integrated over time. This matrix element is the starting point from which we investigate all properties of two-photon decay. We can further evaluate it by writing the electron-photon interaction operator as

$$\hat{R}(\boldsymbol{k}, \boldsymbol{\epsilon}) = \boldsymbol{\alpha}\cdot(\boldsymbol{\epsilon} + G\hat{\boldsymbol{k}})e^{i\boldsymbol{k}\boldsymbol{r}} - Ge^{i\boldsymbol{k}\boldsymbol{r}}, \quad (5)$$

where we introduced an arbitrary gauge parameter G. This parameter is later set to either $G = 0$ for the velocity gauge or $G = \sqrt{(L+1)/L}$ for the length gauge. It is convenient to decompose the interaction operator $\hat{R}$ into spherical tensors. For emission of a photon in the direction $\hat{\boldsymbol{k}} = (\theta, \phi)$, this expansion reads

$$\hat{R}(\boldsymbol{k}, \boldsymbol{\epsilon}) = 4\pi \sum_{pLM} i^{L-|p|}\big[\boldsymbol{\epsilon}\cdot\boldsymbol{Y}^{(p)*}_{LM}(\hat{\boldsymbol{k}})\big]a^{(p)}_{LM}, \quad (6)$$

where $\boldsymbol{Y}^{(p)*}_{LM}$ are vector spherical harmonics and the index p describes electric ($p = 1$), magnetic ($p = 0$), and longitudinal ($p = -1$) multipole fields [3,17]. By inserting this decomposition into Eq. (4) and using the Wigner-Eckart theorem we obtain

$$M_{fi}(\boldsymbol{k}_1, \boldsymbol{\epsilon}_1, \boldsymbol{k}_2, \boldsymbol{\epsilon}_2) = \sum_{p_1L_1M_1}\sum_{p_2L_2M_2} i^{|p_1|+|p_2|-L_1-L_2} \times \big[\boldsymbol{\epsilon_1}^*\cdot\boldsymbol{Y}^{(p_1)}_{L_1M_1}\big]\big[\boldsymbol{\epsilon_2}^*\cdot\boldsymbol{Y}^{(p_2)}_{L_2M_2}\big] \times \widetilde{M}_{fi}(p_1L_1M_1, p_2L_2M_2), \quad (7)$$

where the matrix element for a particular multipole transition (p_1L_1, p_2L_2) is given by

$$\widetilde{M}_{fi}(p_1L_1M_1, p_2L_2M_2) = \sum_{n_\nu\kappa_\nu\mu_\nu} \frac{(4\pi)^2}{\sqrt{(2j_i+1)(2j_\nu+1)}} \times \Bigg[\langle j_f\mu_f L_1M_1|j_\nu\mu_\nu\rangle\langle j_\nu\mu_\nu L_2M_2|j_i\mu_i\rangle \frac{\langle n_f\kappa_f\|a^{(p_1)\dagger}_{L_1}\|n_\nu\kappa_\nu\rangle\langle n_\nu\kappa_\nu\|a^{(p_2)\dagger}_{L_2}\|n_i\kappa_i\rangle}{E_\nu - E_i + \omega_2} + \langle j_f\mu_f L_2M_2|j_\nu\mu_\nu\rangle\langle j_\nu\mu_\nu L_1M_1|j_i\mu_i\rangle \frac{\langle n_f\kappa_f\|a^{(p_2)\dagger}_{L_2}\|n_\nu\kappa_\nu\rangle\langle n_\nu\kappa_\nu\|a^{(p_1)\dagger}_{L_1}\|n_i\kappa_i\rangle}{E_\nu - E_i + \omega_1}\Bigg] \quad (8)$$

and with $\langle n_f \kappa_f \| a_L^{(p)\dagger} \| n_i \kappa_i \rangle$ being the reduced one-photon matrix element [18,19].

With the help of matrix element (7)-(8), we can now calculate observable quantities. For example, the triple differential (in energy and angles) decay rate is given by

$$dW(\omega_1, \Omega_1, \Omega_2, \boldsymbol{\epsilon}_1, \boldsymbol{\epsilon}_2) = e^4 \frac{\omega_1 (E_i - E_f - \omega_1)}{(2\pi)^3} \frac{1}{2j_i + 1} \times \sum_{\mu_i \mu_f} |M_{fi}(\boldsymbol{k}_1, \boldsymbol{\epsilon}_1, \boldsymbol{k}_2, \boldsymbol{\epsilon}_2)|^2 d\Omega_1 d\Omega_2 d\omega_1. \quad (9)$$

Here, we assume that the magnetic sublevels of both the initial and final states, remain unresolved and hence sum over μ_f and average over μ_i. If, moreover, the direction and polarization of the emitted photons are not detected in a particular study, we can obtain the energy-differential rate:

$$\frac{dW}{d\omega_1} = \sum_{\boldsymbol{\epsilon}_1 \boldsymbol{\epsilon}_2} \int \frac{dW}{d\Omega_1 d\Omega_2 d\omega_1} d\Omega_1 d\Omega_2. \quad (10)$$

The integration over the photon angles and the summation over their polarization can be easily performed using Eq. (7). Namely, by inserting the matrix element $M_{fi}(\boldsymbol{k}_1, \boldsymbol{\epsilon}_1, \boldsymbol{k}_2, \boldsymbol{\epsilon}_2)$ into Eqs. (9) and (10) and using the orthonormality relations

$$\sum_{\epsilon} \int d\Omega \left[\boldsymbol{\epsilon}^* \cdot \boldsymbol{Y}_{LM}^{(p)} \right] \left[\boldsymbol{\epsilon} \cdot \boldsymbol{Y}_{L'M'}^{(p')*} \right] = \delta_{pp'} \delta_{LL'} \delta_{MM'}, \quad (11)$$

we obtain

$$dW(\omega_1) = \sum_{p_1 L_1 M_1} \sum_{p_2 L_2 M_2} dW_{p_1 L_1 p_2 L_2}(\omega_1). \quad (12)$$

As seen from this expression, the single differential decay rate can be obtained as the sum of individual multipole contributions

$$dW_{p_1 L_1 p_2 L_2}(\omega_1) = e^4 \frac{\omega_1 (E_i - E_f - \omega_1)}{(2\pi)^3} \frac{1}{2j_i + 1} d\omega_1 \times \sum_{\mu_i \mu_f} |\widetilde{M}_{fi}(p_1, L_1, M_1, p_2, L_2, M_2)|^2 \quad (13)$$

with no interference terms. Finally, by integrating Eq. (12) over the frequency ω_1, we obtain the total decay rate

$$W = \frac{1}{2} \int_0^{E_i - E_f} \frac{dW(\omega_1)}{d\omega_1} d\omega_1, \quad (14)$$

where the factor $1/2$ is introduced to avoid double photon counting (see [10] for more details).

B. Finite basis expansion

As seen from Eq. (8), the evaluation of the two-photon decay rate requires one to perform a summation over all intermediate states $|n_\nu \kappa_\nu \mu_\nu\rangle$ explicitly. Being infinite and running over both bound and continuum states, this summation is not a simple task. In the past, a large number of methods has been proposed to perform this summation. For example, the Coulomb Green's function approach [16,20,21] and various finite basis set methods [4–6] were both successfully applied to perform second-order calculations. In this work, we will also use finite basis sets constructed from B-spline functions. Since B-spline sets in atomic physics have been discussed in the literature [22,23], we restrict ourselves to some basic formulas.

We start our analysis from the usual Dirac equation for the electron in the field of the nucleus. Assuming the potential for the interaction is spherically symmetric, the radial part of this equation can be given by

$$H_\kappa \phi_{n\kappa}(r) = E_{n\kappa} \phi_{n\kappa}(r), \quad (15)$$

where

$$H_\kappa = \begin{pmatrix} V(r) + 1 & -\frac{d}{dr} + \frac{\kappa}{r} \\ \frac{d}{dr} + \frac{\kappa}{r} & V(r) - 1 \end{pmatrix} \quad (16)$$

is the radial Dirac Hamiltonian and

$$\phi_{n\kappa}(r) = \frac{1}{r} \begin{pmatrix} G_{n\kappa}(r) \\ F_{n\kappa}(r) \end{pmatrix} \quad (17)$$

are the radial wave functions. To solve this equation, we approximate these wave functions by

$$\phi_{n\kappa}(r) = \sum_{i=1}^{2N} c_{n\kappa}^i u_\kappa^i(r), \quad (18)$$

where the $u_\kappa^i(r)$ are square-integrable, linearly independent two-component functions that satisfy proper boundary conditions. In order to find the expansion coefficients $c_{n\kappa}^i$, one usually applies the principle of least action $\delta S = 0$ with

$$S = \langle \phi_{n\kappa} | H_\kappa | \phi_{n\kappa} \rangle - E \langle \phi_{n\kappa} | \phi_{n\kappa} \rangle. \quad (19)$$

Inserting in this expression the wave functions (18), the variational condition reduces to the generalized eigenvalue problem

$$K_\kappa^{ik} c_{n\kappa}^k = E_{n\kappa} B_\kappa^{ik} c_{n\kappa}^k, \quad (20)$$

where

$$K_\kappa^{ik} = \left(\langle u_\kappa^i | H_\kappa | u_\kappa^k \rangle + \langle u_\kappa^k | H_\kappa | u_\kappa^i \rangle \right) / 2, \quad (21a)$$

$$B_\kappa^{ik} = \langle u_\kappa^i | u_\kappa^k \rangle. \quad (21b)$$

In order to calculate the K_κ^{ik} and B_κ^{ik} matrix elements, to solve the generalized eigenvalue problem (20) and find the $c_{n\kappa}^i$ coefficients, we have to specify the functions u_κ^i. Following the method by Shabaev *et al.* [22], we choose

$$u_\kappa^i(r) = \begin{pmatrix} \pi^i(r) \\ \frac{1}{2} \left(\frac{d}{dr} + \frac{\kappa}{r} \right) \pi^i(r) \end{pmatrix}, \quad i \leqslant N \quad (22a)$$

$$u_\kappa^i(r) = \begin{pmatrix} \frac{1}{2} \left(\frac{d}{dr} - \frac{\kappa}{r} \right) \pi^{i-N}(r) \\ \pi^{i-N}(r) \end{pmatrix}, \quad i > N, \quad (22b)$$

where $\{\pi^i(r)\}_{i=1}^N$ is the set of B splines on the finite interval $(0, R_{\text{cav}})$. The radius R_{cav} of the finite cavity, in which the ion is enclosed, is chosen large enough to ensure that the wave functions (18) are a good approximation for the real hydrogenic wave functions of the initial and final state. Here, the first and last B splines on the interval are omitted to fulfill the proper boundary conditions [22]: $F_{n\kappa}(0) = 0$ for $\kappa < 0$, $G_{n\kappa}(0) = 0$ for $\kappa > 0$, and $F_{n\kappa}(R_{\text{cav}}) = G_{n\kappa}(R_{\text{cav}}) = 0$. This

particular choice of the functions u_κ^i, by construction (22), avoids the unphysical so-called spurious states which often show up in finite basis methods and slow down the convergence of any calculation.

C. Electron-nucleus interaction potential

In the previous section, we have shown how the hydrogenic Dirac wave functions can be constructed in the framework of a finite basis method. As seen from Eqs. (16), (20), and (21), the practical implementation of this method requires knowledge about the electron nucleus interaction potential. Generally, this potential can be obtained by

$$V(r) = e \int d^3\boldsymbol{r}' \frac{\rho(r')}{|r - r'|}, \tag{23}$$

where $\rho(r')$ is the nuclear charge density. In the present study, we will consider a few models of $\rho(r')$ to better understand the nuclear effects on the two-photon decay rate. The most naive approach is the pointlike nucleus represented by the charge distribution

$$\rho_{\rm pnt}(\boldsymbol{r}) = \rho_0 \delta(\boldsymbol{r}), \tag{24}$$

which leads to the usual Coulomb potential $V = \alpha Z/r$.

In order to account for the effects of the finite nuclear size, we will either model the nucleus as a homogeneously charged sphere

$$\rho_{\rm sph}(\boldsymbol{r}) = \rho_0 \Theta(R_{\rm sph} - r), \tag{25}$$

where $R_{\rm sph}$ is related to the root-mean-square charge radius by $R_{\rm sph} = \sqrt{5/3}R$, or as a Fermi distribution

$$\rho_{\rm Fermi}(\boldsymbol{r}) = \frac{\rho_0}{1 + \exp[(r - c)/a]}. \tag{26}$$

For the latter $a = 2.3/(4 \ln 3)$ fm and the parameter c is given by the approximate formula

$$c \approx \tfrac{5}{3}R^2 - \tfrac{7}{3}a^2\pi^2, \tag{27}$$

see [24,25]. For both nuclear models, (25) and (26), the nuclear radius is taken from Ref. [26].

Apart from the finite nuclear size effects, other phenomena can also influence the two-photon decay rate of hydrogenlike ions. For example, the interaction of the electron with the quantum vacuum may affect the wave functions [27,28], the energy levels [25], and the transition operators [11–13] and, hence, the decay rate. In the one-loop approximation, two QED contributions are usually considered: vacuum polarization and self-energy. While the complete treatment of these two corrections to the second-order amplitude is a very complicated task, the vacuum polarization to the leading order $\alpha(\alpha Z)^2$ can be described by an effective Uehling potential. The corresponding diagrams can be obtained by vacuum-polarization insertions in the initial and final wave functions and the propagator between the two photon emissions (cf. Fig. 1). The diagrams, which cannot be accounted for by an effective potential, such as photon-vacuum-polarization-loop or two-photon-vacuum-polarization-loop diagrams, vanish in the free-loop approximation, and, therefore, contribute beyond the leading order. Thus, the leading-order contributions of diagrams with the ordinary vacuum-polarization insertions can be treated by solving the Dirac equation with the Uehling potential

$$V_{\rm Uehl}(r) = -\alpha Z \frac{2\alpha}{3\pi} \int_0^\infty dr' 4\pi r' \rho(r') \times \int_1^\infty dt \left(1 + \frac{1}{2t^2}\right) \frac{\sqrt{t^2 - 1}}{t^2} \times \frac{\exp(-2|r - r'|t) - \exp(-2|r + r'|t)}{4rt}, \tag{28}$$

where the nuclear charge distribution $\rho(r')$ is assumed to be spherically symmetric. To account for both the vacuum polarization and the finite nuclear size effects, we sum $V_{\rm Uehl}$ and the potential resulting from Eq. (25) or (26), respectively. The technical details of these calculations will be discussed in the next section.

III. COMPUTATIONAL DETAILS

The present work aims to investigate the finite nuclear size and QED effects on the two-photon decay rates of hydrogenlike ions. These effects are rather small requiring a high accuracy of our calculations. Namely, their numerical uncertainty should be remarkably lower compared to the size of the discussed effects. As usual in atomic structure calculations, we verify the accuracy of the computations by testing the gauge invariance of the decay rates. Following our discussion above, calculations within the so-called velocity and length gauge are compared. For all results presented in the next section, the relative difference of the energy differential decay rates obtained in these two gauges is smaller than 10^{-13}. It is not a simple task to reach such high accuracy, especially in the low-Z regime. The main reason for that is the standard LAPACK [29] routines which are commonly utilized to solve generalized eigenvalue problems and are designed to use double-precision arithmetic. They suffer, hence, a loss of numerical significance for large diagonally dominant matrices [5]. In order to overcome this problem, we developed a B-spline code using the C++ template library Eigen [30] which makes it possible to solve the generalized eigenvalue problem with arbitrary precision.

When calculating the total decay rates, we face another difficulty that lowers the gauge invariance and, hence, accuracy of our calculations: The well-known problem of intermediate-state resonances. This problem does not arise for $2s_{1/2} \to 1s_{1/2}$ and $2p_{1/2} \to 1s_{1/2}$ transitions for pointlike nuclei, because of the degeneracy of the $2s_{1/2}$ and $2p_{1/2}$ states. However, the degeneracy is lifted when dealing with finite nuclear size, which leads to the fact that the $2s_{1/2} \to 1s_{1/2}$ decay may proceed via the real intermediate $2p_{1/2}$ state. The existence of this intermediate state might be observed as a resonance in the energy differential decay rate, as seen from Fig. 2. The appearance of such a resonance makes the integration over the photon energy and, hence, the calculation of the total rates cumbersome as was discussed in the literature [31,32]. In this work, we follow the approach proposed by Labzowsky *et al.* [32] and introduce the finite linewidth of the resonance state to the electron propagator in a small interval around the divergent resonance. For example in Fig. 2, this procedure is illustrated by the orange dashed line for the

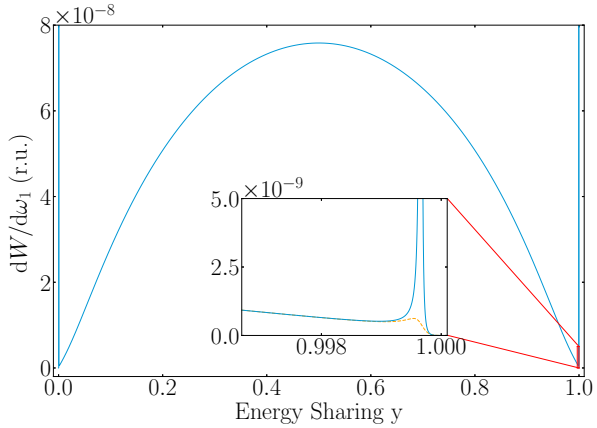

FIG. 2. Energy differential decay rate in relativistic units (r.u.) for the $2s_{1/2} \to 1s_{1/2} + E1E1$ transition in hydrogenlike uranium as a function of the energy sharing $y = \omega_1/(\omega_1 + \omega_2)$. The resonances close to the edges are either untreated (blue solid line) or rendered finite with the method by Labzowsky *et al.* [32] (orange dashed line).

$2s_{1/2} \to 1s_{1/2} + E1E1$ transition in hydrogenlike uranium. Of course, this method leads to the loss of gauge invariance in the small interval. However, since the resonances are located near the edges of the spectral distribution, for example at $y = \omega_1/(\omega_1 + \omega_2) = 0.000\,34$ and $y = 0.999\,66$ for U^{91+}, the violation of the gauge invariance does not affect the total rate significantly. The results of our calculations show that introducing an artificial linewidth to fix the resonance problem does not result in a violation of the gauge invariance above the level of 10^{-7} for the total rate. Therefore, all digits presented in the next section are still significant.

Yet another source of uncertainty of the two-photon calculations is imprecise knowledge about the nuclear size R. With the compilation of Angeli and Marinova [26], this leads to relative uncertainties in the calculation of the decay rates that do not exceed 10^{-8}. We confirm this level of accuracy also when comparing calculations performed in the framework of the two nuclear models, namely, the Fermi and solid sphere models.

Finally, to verify the correct implementation of the B-spline method and the electron-nucleus interaction potentials, we present in Table I the binding energies for the pointlike nucleus and the energy shift due to finite nuclear size and vacuum polarization effects. These energies are obtained as the eigenvalues of the generalized eigenvalue problem (20) and, as seen from the table, show a good agreement with the results from Yerokhin and Shabaev [33].

In summary, we can assure one that all digits presented in the next section are meaningful in our approach in which finite nuclear size and vacuum polarization effects are taken into account. However, other corrections that are beyond the scope of this study may affect the decay rates at the same order of magnitude as the considered effects. For example, it is known that in the nonrelativistic limit, the self-energy contribution is even larger than that of the vacuum polarization. In particular, this self-energy correction reduces the $2s \to 1s + 2\gamma$ decay rate by 0.000 25% for hydrogen and 0.038% for hydrogenlike calcium [15]. However, the behavior for heavy ions remains unknown.

TABLE I. Binding energies for a pointlike nucleus and energy shifts due to finite nuclear size and vacuum polarization effects in units of eV. Results are presented for the $1s_{1/2}$, $2s_{1/2}$, and $2p_{1/2}$ states of hydrogenlike ions with nuclear charge Z. Brackets denote powers of 10.

Z	$E_{\rm pnt}$	$\Delta E_{\rm fnt}$	$\Delta E_{\rm Uehl}$
		$1s_{1/2}$	
1	−13.6059	4.99(−9)	−8.90(−7)
	−13.6059[b]	4.99(−9)[a]	−8.90(−7)[a]
40	−22253.68	0.516	−2.084
	−22253.68[b]	0.516[a]	−2.083[a]
92	−132279.93	198.7	−93.8
	−132279.93[b]	199.0[a]	−93.6[a]
		$2s_{1/2}$	
1	−3.4015	6.24(−10)	−1.11(−7)
	−3.4015[b]	6.25(−10)[a]	−1.11(−7)[a]
40	−5594.04	0.0696	−0.277
	−5594.04[b]	0.0696[a]	−0.277[a]
92	−34215.48	37.81	−16.50
	−34215.48[b]	37.71[a]	−16.46[a]
		$2p_{1/2}$	
1	−3.4015	0.0	−1.3(−12)
	−3.4015[b]	0.0[a]	−1.3(−12)[a]
40	−5594.04	0.0012	−0.0068
	−5594.04[b]	0.0012[a]	−0.0068[a]
92	−34215.48	4.41	−2.91
	−34215.48[b]	4.42[a]	−2.91[a]

[a] Yerokhin and Shabaev [33].
[b] Analytical formula from relativistic Dirac theory.

IV. RESULTS AND DISCUSSION

A. $2s_{1/2} \to 1s_{1/2}$ two-photon transition

By using Eqs. (7)–(14) and the finite basis set method, discussed in Sec. II B, we calculate the total rates for the two-photon decay of hydrogenlike ions. We start our discussion with the well-known $2s_{1/2} \to 1s_{1/2} + 2\gamma$ transition. In leading order, this decay proceeds with the emission of two electric dipole photons. The total rates $W_{E1,E1}$ for this $2E1$ transition are displayed in Table II for nuclear charges ranging from $Z = 1$ to $Z = 92$ and for different electron-nucleus interaction potentials. In particular, calculations have been performed for the pointlike and finite-size nucleus and by accounting for the vacuum polarization as described by the Uehling potential (28). Moreover, by following the well-known nonrelativistic Z behavior [34], we present our results divided by Z^6. For the naive pointlike nuclear model, a good agreement with the previous calculations by Goldman [4] and Filippin *et al.* [6] is obtained. Here, we agree up to the level of approximately 10^{-7} and 10^{-9}, respectively. We note moreover, a misprint in the first digit of the value for $Z = 20$ of Goldman [4].

In order to investigate the effects of the finite nuclear size for the $2s_{1/2} \to 1s_{1/2} + 2E1$ decay rates, we performed calculations also for the hard-sphere and Fermi distribution. As mentioned already above, both models agree on the level of 10^{-8} and are presented in the third column of Table II. As seen from the table, the finite nuclear size reduces the decay rates by 2.79×10^{-8}% for neutral hydrogen and up to 0.0092%

TABLE II. Total two-photon $2s_{1/2} \to 1s_{1/2}$ decay rates for hydrogenlike ions with nuclear charge Z in units Z^6 s^{-1}. Calculations have been performed for the $E1E1$ multipole channel and for a pointlike nucleus ($V_{\rm pnt}$), a finite-sized nucleus ($V_{\rm fnt}$), and a finite nucleus with additional Uehling potential ($V_{\rm fnt} + V_{\rm Uehl}$).

Z	$V_{\rm pnt}$	$V_{\rm fnt}$	$V_{\rm fnt} + V_{\rm Uehl}$
1	8.2290615	8.2290615	8.2290619
	8.2290615[a]	8.22906[c]	
	8.2290626[b]		
20	8.1174024	8.1173852	8.1175410
	9.1174035[b]	8.1095[c]	
40	7.8092601	7.8091196	7.8097303
	7.8092601[a]	7.8013[c]	
	7.8092612[b]		
60	7.3446473	7.344077	7.3453658
	7.3446482[b]	7.3365[c]	
80	6.7428868	6.74157	6.74347
	6.7428876[b]	6.7348[c]	
92	6.3096615	6.30908	6.31098
	6.3096618[a]	6.3026[c]	
	6.3096623[b]		

[a]Filippin *et al.* [6].
[b]Goldman [4]; there seems to be a misprint in the value for $Z = 20$.
[c]Labzowsky *et al.* [10].

for hydrogenlike uranium ions which is in good agreement with the findings from Parpia and Johnson [9] and Labzwosky *et al.* [10] within their estimated error. The reduction can be understood qualitatively by analyzing the nonrelativistic hydrogenic Z^6 scaling of the transition rate. This scaling law implies that a stronger electron-nucleus interaction potential results in an increase of the decay rate. Since replacing the pointlike with a finite-size nucleus weakens the interaction potential, the decay rate gets reduced.

Yet another correction that may affect the $2s_{1/2} \to 1s_{1/2} + 2\gamma$ decay rate is the vacuum polarization which is approximated by the Uehling potential. As seen from the fourth column of Table II, this correction increases the decay rate by 4.96×10^{-6}% for hydrogen and 0.03% for U^{91+}. Qualitatively, the enhancement can be again understood from the nonrelativistic limit in which a stronger coupling potential increases the decay rate. As seen from Eq. (28), the vacuum polarization leads to a stronger binding of the electron in the potential of the nucleus and, hence, results in the larger decay rate.

By comparing the third and fourth columns of Table II, we see that the vacuum polarization correction to the total decay rate is always larger than the one obtained from the finite nuclear size. This is especially surprising since the transition energies are known to be stronger influenced by the finite nuclear size in the high-Z regime as also seen from Table I. To explain this unexpected behavior, we have to look again at Eq. (13). As already explained above, for the $2s_{1/2} \to 1s_{1/2} + 2E1$ transition, the finite nuclear size reduces the transition energies and enhances the matrix elements. In contrast, the vacuum polarization acts just in the opposite direction and, similar to the finite nuclear size correction, the QED

TABLE III. Total two-photon $2s_{1/2} \to 1s_{1/2}$ decay rates for hydrogenlike ions with nuclear charge Z in units Z^6 s^{-1}. Results have been obtained for a pointlike nucleus ($V_{\rm point}$), a finitely sized nucleus ($V_{\rm finite}$), and a finite nucleus with additional Uehling potential ($V_{\rm fnt} + V_{\rm Uehl}$). Moreover, we have performed the summation over all allowed multipole channels p_1L_1, p_2L_2 for $L_1, L_2 = 1 \ldots 4$.

Z	$V_{\rm point}$	$V_{\rm finite}$	$V_{\rm fnt} + V_{\rm Uehl}$
1	8.2290615	8.2290615	8.2290619
	8.2290615[a]		
	8.2290626[b]		
20	8.1174454	8.1174282	8.1175840
	8.1174464[a]		
	8.1174466[b]		
40	7.8099289	7.8097883	7.8103993
	7.8099289[a]		
	7.8099299[b]		
60	7.3479098	7.347339	7.3486296
	7.3479098[a]		
	7.3479109[b]		
80	6.7528665	6.75154	6.75345
	6.7528660[a]		
	6.7528675[b]		
92	6.3269332	6.32633	6.32821
	6.326931[b]		
	6.3269340[a]		

[a]Filippin *et al.* [6].
[b] Goldman [4].

contributions to the matrix element $\widetilde{M}_{fi}$ and energy prefactor partially cancel each other. However, this cancellation is less pronounced for the vacuum polarization case, thus resulting in the stronger sensitivity of the results to the Uehling correction.

So far, we discussed the leading $2E1$ channel of the $2s_{1/2} \to 1s_{1/2} + 2\gamma$ transition. Owing to the selection rules, the other—much weaker—channels can also contribute to this decay. In order to investigate the role of the higher-order multipole contributions, we calculated the total decay rate $W = \sum_{p_1L_1p_2L_2} W(p_1L_1, p_2L_2)$ where the summation over L_1 and L_2 runs up to $L_{\rm max} = 4$. The results of these calculations are shown in Table III again for a point nucleus and including the finite nuclear size and vacuum polarization corrections. As seen from the table, the contributions of both corrections are qualitatively similar to what was observed for the leading $2E1$ channel. In particular, the total two-photon decay rates are reduced by the finite nuclear size and enhanced if the vacuum polarization is taken into account.

B. $2p_{1/2} \to 1s_{1/2}$ two-photon transition

Besides the well-known $2s_{1/2} \to 1s_{1/2} + 2\gamma$ decay, we also apply our theory to discuss the $2p_{1/2} \to 1s_{1/2} + 2\gamma$ transition. In the leading order, this decay may proceed via $E1M1$ or $E1E2$ channels. The results for the $E1M1$ channel are presented in Table IV, again for a pointlike and finite-size nucleus as well as accounting for the Uehling correction. The decay rates are obtained in the range from $Z = 1$ to $Z = 92$ and are rescaled as Z^8 as suggested by the nonrelativistic limit [10].

TABLE IV. Total two-photon $2p_{1/2} \to 1s_{1/2}$ decay rates for hydrogenlike ions with nuclear charge Z in units $Z^8 \times 10^{-6}$ s^{-1}. Calculations have been performed for the $E1M1$ multipole channel and for a pointlike nucleus ($V_{\rm pnt}$), a finite-sized nucleus ($V_{\rm fnt}$), and a finite nucleus with additional Uehling potential ($V_{\rm fnt} + V_{\rm Uehl}$).

Z	$V_{\rm pnt}$	$V_{\rm fnt}$	$V_{\rm fnt} + V_{\rm Uehl}$
1	9.6766569 9.6766569[a]	9.6766569 9.667[b]	9.6766592
20	9.5561970	9.5561068 9.543[b]	9.5569117
40	9.1973052 9.1973052[a]	9.1966168 9.186[b]	9.1994459
60	8.6260732	8.6231951	8.6288466
80	7.9316051	7.9211520 7.910[b]	7.9307704
92	7.5541404 7.5541404[a]	7.5275515 7.519[b]	7.5416695

[a]Filippin *et al.* [6].
[b]Labzowsky *et al.* [10].

TABLE V. Total two-photon $2p_{1/2} \to 1s_{1/2}$ decay rates for hydrogenlike ions with nuclear charge Z in units $Z^8 \times 10^{-6}$ s^{-1}. Calculations have been performed for the $E1E2$ multipole channel and for a pointlike nucleus ($V_{\rm pnt}$), a finite-sized nucleus ($V_{\rm fnt}$), and a finite nucleus with additional Uehling potential ($V_{\rm fnt} + V_{\rm Uehl}$).

Z	$V_{\rm pnt}$	$V_{\rm fnt}$	$V_{\rm fnt} + V_{\rm Uehl}$
1	6.6117981 6.6117981[a]	6.6117981 6.605[b]	6.6118003
20	6.5202286	6.5201386 6.516[b]	6.5209400
40	6.2446748 6.2446748[a]	6.2439316 6.238[b]	6.2469332
60	5.7832261	5.7797060	5.7862409
80	5.1262923	5.1123097 5.107[b]	5.1237402
92	4.6272865 4.6272865[a]	4.5952682 4.591[b]	4.6101315

[a]Filippin *et al.* [6].
[b]Labzowsky *et al.* [10].

Similar to before, we start the discussion of our results from the finite nuclear size correction. As seen from the table, this correction reduces the decay rate as was also observed for the $2s_{1/2} \to 1s_{1/2} + 2\gamma$ transition. In contrast to that transition, however, the reduction of the $2p_{1/2} \to 1s_{1/2} + E1M1$ decay rate is significantly stronger ranging from 1.34×10^{-7}% for hydrogen to 0.352% for hydrogenlike uranium. Once more, this can be explained by the analysis of the nonrelativistic scaling behavior of the decay rate. In comparison to the $2s_{1/2} \to 1s_{1/2} + E1E1$ transition, one of the $E1$ photons is replaced by an $M1$ photon for the $2p_{1/2} \to 1s_{1/2} + E1M1$ decay and, therefore, the rate scales with Z^8 instead of Z^6. Hence, the decay rate is much more sensitive to changes in the electron-nucleus interaction potential resulting in the larger effect.

As seen from the fourth column of Table IV, the Uehling contribution increases the decay rates between 2.39×10^{-5}% and 0.187%. The overall larger effect, compared to the $2s_{1/2} \to 1s_{1/2} + 2\gamma$ transition, can be again explained by the scaling behavior.

The other leading channel that contributes to the $2p_{1/2} \to 1s_{1/2} + 2\gamma$ decay is the $E1E2$ transition for which the total rates are shown in Table V. This multipole transition exhibits the same Z-scaling law and also generally the same behavior with respect to the corrections due to the finite-size nucleus and vacuum polarization as was observed for the $E1M1$ channel. For the $E1E2$ channel, however, the decay is even more strongly affected by the finite nuclear size and QED effects which may reach, for the decay of hydrogenlike uranium, a reduction by 0.692% and enhancement by 0.322%, respectively.

Similar to before, we also investigate the total $2p_{1/2} \to 1s_{1/2} + 2\gamma$ decay rate by including higher-order multipole terms up to $L_{\rm max} = 4$. The total rates for the pointlike and finite nucleus as well as for the additional Uehling correction are shown in Table VI. As seen from the table, these corrections generally show the same behavior as for the $E1M1$ and $E1E2$ channel. For U^{91+} ions, they lead to a reduction of the total rate by 0.484% due to the finite nuclear size and enhancement by 0.239% due to the vacuum polarization.

V. SUMMARY AND OUTLOOK

In conclusion, we presented a theoretical study of the two-photon decay of hydrogenlike ions. Special attention was paid to the total rates obtained upon integration over the energies and directions of the emitted photons. In order to calculate these total decay rates, we have used the framework of quantum electrodynamics. The use of QED theory has allowed us to naturally account for the finite nuclear size and vacuum polarization corrections. In order to study the size of these corrections, high precision calculations have been performed for the $2s_{1/2} \to 1s_{1/2} + 2\gamma$ and $2p_{1/2} \to 1s_{1/2} + 2\gamma$

TABLE VI. Total two-photon $2p_{1/2} \to 1s_{1/2}$ decay rates for hydrogenlike ions with nuclear charge Z in units $Z^8 \times 10^{-6}$ s^{-1}. Results have been obtained for a pointlike nucleus ($V_{\rm pnt}$), a finitely sized nucleus ($V_{\rm fnt}$), and a finite nucleus with additional Uehling potential ($V_{\rm fnt} + V_{\rm Uehl}$). Moreover, we have performed the summation over all allowed multipole channels p_1L_1, p_2L_2 for $L_1, L_2 = 1 \ldots 4$.

Z	$V_{\rm pnt}$	$V_{\rm fnt}$	$V_{\rm fnt} + V_{\rm Uehl}$
1	16.288455 16.288455[a]	16.288455	16.288460
20	16.076447	16.076267	16.077873
40	15.442308 15.442308[a]	15.440876	15.446707
60	14.410849	14.404450	14.416639
80	13.062372	13.037919	13.058982
92	12.188751 12.188750[a]	12.130067	12.159084

[a]Filippin *et al.* [6].

two-photon decay of hydrogenlike ions in the range from $Z = 1$ to $Z = 92$. Our results have shown that these two well-established transitions are affected differently by the QED and finite nuclear size effects. Particularly, both effects are more pronounced for the $2p_{1/2} \to 1s_{1/2} + 2\gamma$ case. For example, the transition rate in U^{91+} is reduced by 0.484% by the finite nuclear size and enhanced by 0.239% by the Uehling correction. For the $2s_{1/2} \to 1s_{1/2} + 2\gamma$ decay of hydrogenlike uranium, in contrast, these two corrections are just 0.0092% and 0.03%, respectively.

The finite nuclear size and QED corrections discussed in this paper are too small in order to be observed in present-day two-photon experiments. They might be significantly increased, however, when replacing the usual electronic ions by muonic systems. The high-precision B-spline approach developed in the present work can be easily extended to the transition in such muonic ions. The study of two-photon decay of muonic ions is currently under development and its results will be published in a future work.

ACKNOWLEDGMENTS

This work has been supported by the GSI Helmholtz Centre for Heavy Ion Research under the Project No. BSSURZ1922 and by the DFG under the Project No. SU658/4-1.

[1] M. Göppert-Mayer, Über elementarakte mit zwei quantensprüngen, Ann. Phys. **401**, 273 (1931).
[2] W. R. Johnson, Radiative Decay Rates of Metastable One-Electron Atoms, Phys. Rev. Lett. **29**, 1123 (1972).
[3] S. P. Goldman and G. W. F. Drake, Relativistic two-photon decay rates of $2s_{1/2}$ hydrogenic ions, Phys. Rev. A **24**, 183 (1981).
[4] S. P. Goldman, Generalized Laguerre representation: Application to relativistic two-photon decay rates, Phys. Rev. A **40**, 1185 (1989).
[5] P. Amaro, A. Surzhykov, F. Parente, P. Indelicato, and J. P. Santos, Calculation of two-photon decay rates of hydrogen-like ions by using B-polynomials, J. Phys. A: Math. Theor. **44**, 245302 (2011).
[6] L. Filippin, M. Godefroid, and D. Baye, Relativistic two-photon decay rates with the Lagrange-mesh method, Phys. Rev. A **93**, 012517 (2016).
[7] Z. Fried and A. D. Martin, Center-of-mass effect on electromagnetic transition rates in mesic atoms, Il Nuovo Cimento (1955–1965) **29**, 574 (1963).
[8] G. W. F. Drake, Spontaneous two-photon decay rates in hydrogenlike and heliumlike ions, Phys. Rev. A **34**, 2871 (1986).
[9] F. A. Parpia and W. R. Johnson, Radiative decay rates of metastable one-electron atoms, Phys. Rev. A **26**, 1142 (1982).
[10] L. N. Labzowsky, A. V. Shonin, and D. A. Solovyev, QED calculation of $E1M1$ and $E1E2$ transition probabilities in one-electron ions with arbitrary nuclear charge, J. Phys. B: At., Mol. Opt. Phys. **38**, 265 (2005).
[11] J. Sapirstein, K. Pachucki, and K. T. Cheng, Radiative corrections to one-photon decays of hydrogenic ions, Phys. Rev. A **69**, 022113 (2004).
[12] J. Sapirstein and K. T. Cheng, Calculation of radiative corrections to $E1$ matrix elements in the neutral alkali metals, Phys. Rev. A **71**, 022503 (2005).
[13] A. V. Volotka, D. A. Glazov, G. Plunien, V. M. Shabaev, and I. I. Tupitsyn, Radiative corrections to the magnetic-dipole transition amplitude in B-like ions, Eur. Phys. J. D **38**, 293 (2006).
[14] S. G. Karshenboim and V. G. Ivanov, Radiative corrections to the light muonic atoms decay rate, Phys. Lett. A **235**, 375 (1997).
[15] Ulrich D. Jentschura, Self-energy correction to the two-photon decay width in hydrogenlike atoms, Phys. Rev. A **69**, 052118 (2004).
[16] P. J. Mohr, G. Plunien, and G. Soff, QED corrections in heavy atoms, Phys. Rep. **293**, 227 (1998).
[17] N. L. Manakov, A. V. Meremianin, and A. F. Starace, Multipole expansions of irreducible tensor sets and some applications, J. Phys. B: At., Mol. Opt. Phys. **35**, 77 (2001).
[18] I. P. Grant, *Relativistic Quantum Theory of Atoms and Molecules: Theory and Computation*, Springer Series on Atomic, Optical, and Plasma Physics (Springer-Verlag, Berlin, Heidelberg, 2006).
[19] I. P. Grant, Gauge invariance and relativistic radiative transitions, J. Phys. B **7**, 1458 (1974).
[20] R. A. Swainson and G. W. F. Drake, A unified treatment of the non-relativistic and relativistic hydrogen atom II: the Green functions, J. Phys. A: Math. Gen. **24**, 95 (1991).
[21] P. Koval and S. Fritzsche, Relativistic wave and Green's functions for hydrogen-like ions, Comput. Phys. Commun. **152**, 191 (2003).
[22] V. M. Shabaev, I. I. Tupitsyn, V. A. Yerokhin, G. Plunien, and G. Soff, Dual Kinetic Balance Approach to Basis-Set Expansions for the Dirac Equation, Phys. Rev. Lett. **93**, 130405 (2004).
[23] H. Bachau, E. Cormier, P. Decleva, J. E. Hansen, and F. Martín, Applications of B-splines in atomic and molecular physics, Rep. Prog. Phys. **64**, 1815 (2001).
[24] W. R. Johnson, *Atomic Structure Theory: Lectures on Atomic Physics* (Springer-Verlag, Berlin, Heidelberg, 2007).
[25] V. A. Yerokhin, Nuclear-size correction to the Lamb shift of one-electron atoms, Phys. Rev. A **83**, 012507 (2011).
[26] I. Angeli and K. P. Marinova, Table of experimental nuclear ground state charge radii: An update, At. Data Nucl. Data Tables **99**, 69 (2013).
[27] J. Holmberg, A. N. Artemyev, A. Surzhykov, V. A. Yerokhin, and Th. Stöhlker, QED corrections to radiative recombination and radiative decay of heavy hydrogenlike ions, Phys. Rev. A **92**, 042510 (2015).
[28] N. S. Oreshkina, H. Cakir, B. Sikora, V. A. Yerokhin, V. Debierre, Z. Harman, and C. H. Keitel, Self-energy-corrected Dirac wave functions for advanced QED calculations in highly charged ions, Phys. Rev. A **101**, 032511 (2020).
[29] E. Anderson, Z. Bai, C. Bischof, S. Blackford, J. Demmel, J. Dongarra, J. Du Croz, A. Greenbaum, S. Hammarling, A. McKenney, and D. Sorensen, *LAPACK users' guide*, 3rd ed. (Society for Industrial and Applied Mathematics, Philadelphia, PA, 1999).

[30] G. Guennebaud, B. Jacob *et al.*, Eigen v3, 2010, http://eigen.tuxfamily.org.

[31] U. D. Jentschura and A. Surzhykov, Relativistic calculation of the two-photon decay rate of highly excited ionic states, Phys. Rev. A **77**, 042507 (2008).

[32] L. Labzowsky, D. Solovyev, and G. Plunien, Two-photon decay of excited levels in hydrogen: The ambiguity of the separation of cascades and pure two-photon emission, Phys. Rev. A **80**, 062514 (2009).

[33] V. A. Yerokhin and V. M. Shabaev, Lamb shift of $n = 1$ and $n = 2$ states of hydrogen-like atoms, $1 \leqslant Z \leqslant 110$, J. Phys. Chem. Ref. Data **44**, 033103 (2015).

[34] S. Klarsfeld, Radiative decay of metastable hydrogenic atoms, Phys. Lett. A **30**, 382 (1969).